Establishment of a Simple, Reproducible, and Long-lasting Hind Limb Animal Model of Lymphedema

Yuichi Morita, MD[*†‡]
Naoaki Sakata, MD[*†§]
Ryo Kawakami, MSc[*†§]
Masayuki Shimizu, MD[*†‡]
Gumpei Yoshimatsu, MD[*†§]
Hideichi Wada, MD[‡§]
Shohta Kodama, MD[*†§]

Background: Lymphedema is an intractable disease for which there is currently no established curative therapy. A reliable and long-lasting lymphedema model is essential for development of better treatments. In this study, we aimed to establish a simple, reproducible and long-lasting mouse model of lymphedema.
Methods: Our model is characterized by a combination of a circumferential skin incision in the femoral region, complete dissection of regional lymph nodes, and ablation of the inguinal route in the femoral region. The characteristics of the lymphedema were evaluated and compared with those of two other models. One of these models involved dissection of the subiliac, popliteal, and sciatic lymph nodes (model A) and the other excision of the subiliac, popliteal, and sciatic lymph nodes with cauterization of lymphatic vessels and closure without a skin excision (model B).
Results: Although the lymphedema in models A and B resolved spontaneously, that in the new model lasted for a month with increases in femoral circumference and hind limb volume, thickening of the skin, especially subcutaneous tissue, and congestion of peripheral lymphatic vessels. Furthermore, this model could be used for assessing the therapeutic effects of syngeneic mesenchymal stem cell transplantation. The average operation time for the new model was 14.4 ± 1.3 minutes.
Conclusion: Long-lasting lymphedema can be achieved by our new model, making it suitable for assessing therapies for lymphedema. *(Plast Reconstr Surg Glob Open 2023; 11:e5243; doi: 10.1097/GOX.0000000000005243; Published online 7 September 2023.)*

INTRODUCTION

Lymphedema is lymphatic stasis in the subcutaneous tissue caused by impairment of the lymphatic system. Although lymphedema is generally not life-threatening, management of this condition is crucial because it impairs the quality of life of affected individuals. The current standard therapy for lymphedema is a combination of decompression therapies[1]; however, the therapeutic effects are unsatisfactory.[2] The potentially useful radical therapy of mesenchymal stem cell (MSC) transplantation has been discussed.[3,4]

Appropriate and reliable animal models that reproduce the pathophysiology of lymphedema are essential for the development of better treatments and assessment of their usefulness. However, the published models are limited in that the lymphedema is short lived,[5] resolving spontaneously over time with most available surgical models.[6] Irradiation frequently prolongs lymphedema; however, lymphedema induced by irradiation models is unstable.[7] Furthermore, irradiation injures healthy soft tissue and skin, interfering with tissue repair.[1,8] Therefore, a better animal model with long-lasting lymphedema that can be created by a simple procedure would contribute to establishing curative and radical therapy for this disease and alleviate many patients' troublesome symptoms. In this study, we aimed to establish a simple and reproducible mouse model of long-lasting lymphedema.

METHODS

Animals and Ethical Considerations

Eight-week-old male C57BL/6J mice (Charles River Laboratories, Yokohama, Japan) were used as hind limb

Disclosure statements are at the end of this article, following the correspondence information.

Related Digital Media are available in the full-text version of the article on www.PRSGlobalOpen.com.

lymphedema animal models. They were carefully monitored and freely fed a normal diet. The care of animals and experimental procedures in this study were in accordance with the Principles of Laboratory Animal Care according to the Guide for the Care and Use of Laboratory Animals eighth edition (National Institutes of Health publication, 2011). The experimental protocol was approved by the Animal Care and Use Committee of Fukuoka University (Approval number: 2113110).

Procedure for Inducing Hind Limb Lymphedema in Our New Model

We postulated that complete elimination of major lymph routes and accompanying lymph nodes would be crucial in establishing a stable lymphedema model. Therefore, we completely eliminated the three major lymphatic routes (subiliac, popliteal, and inguinal routes) with their regional lymph nodes (Fig. 1A). We also made
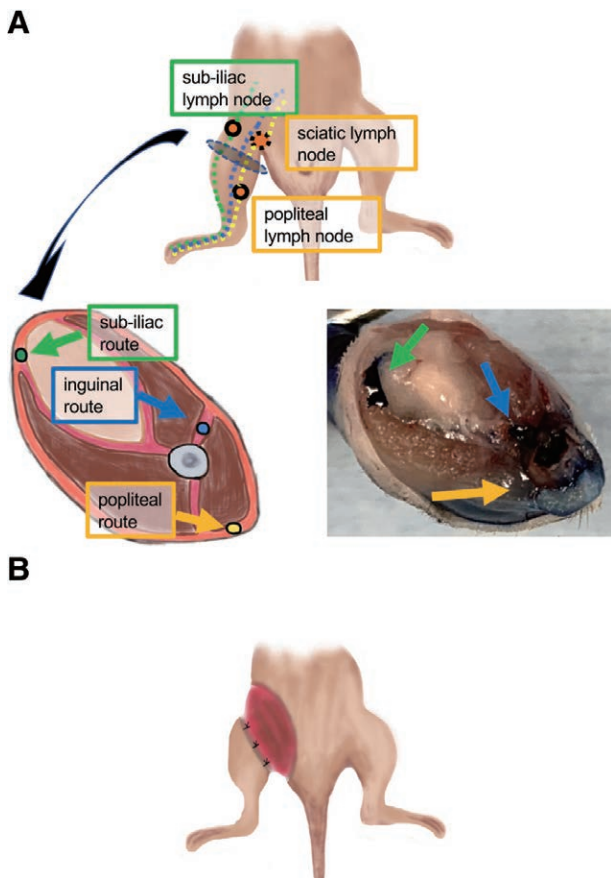
Fig. 1. Anatomy of lymphatic vessels in the hind limb and postoperative view of the new model. A, Anatomy of lymphatic vessels in the hind limb. Top: Diagrammatic representation of the three major lymphatic routes, namely the subiliac (green dotted line), popliteal (yellow dotted line), and inguinal (blue dotted line) routes. Bottom figure on the left: Diagrammatic representation of a cross-section of the femoral region: subiliac route (green), popliteal route (yellow) and inguinal route (blue) routes. Bottom figure on the right: Diagrammatic representation of a cross-section of the femoral region labeled with 1% Evans blue. B, Postoperative views of this surgery.

Takeaways

Question: Is our new lymphedema animal model, characterized by a combination of a circumferential femoral skin incision, regional lymph node dissection, and ablation of the inguinal route, acceptable as a long-lasting lymphedema model and available for assessing therapies for lymphedema?

Findings: Lymphedema in our model lasted for a month with increases in femoral circumference and hind limb volume, thickening of the skin and congestion of peripheral lymphatic vessels. Furthermore, this model could be used for assessing the therapeutic effects of syngeneic mesenchymal stem cell transplantation.

Meaning: Long-lasting lymphedema can be achieved by our new model, making it suitable for assessing therapies for lymphedema.

a circumferential skin incision in the inguinal region to interrupt the major lymphatic routes (Fig. 1B).

The procedure of our new lymphedema model is shown in supplemental Digital Content 1. [**See figure, Supplemental Digital Content 1**, which displays the procedure for creating the new model for hind limb lymphedema. First row: Evans blue is injected subcutaneously into the right hind limb (left panel). The lymph vessels and nodes are labeled (middle panel). A circumferential skin incision is made in the inguinal region (right panel). Second row: the contrast-enhanced subiliac, popliteal and sciatic lymph nodes (yellow arrows) excised using electrocautery. Third row: the lymphatic vessels are also cauterized simultaneously. The circumferential gap in the skin of the inguinal region is approximately 10 mm wide. The proximal side of the skin transection is cauterized and the distal side fixed to myofascia using 6-0 nylon sutures. Fourth panel: postoperative views of this surgery, **http://links.lww.com/GOX/A9**.]

The mice were anesthetized using isoflurane (Fujifilm Wako Pure Chemical Corporation, Osaka, Japan). First, Evans blue (Fujifilm Wako Pure Chemical Corporation) was injected subcutaneously into the right hind limb, revealing the three lymphatic routes. The procedure to induce hind limb lymphedema was then performed. A circumferential skin incision was made in the inguinal region and electrocautery used to excise the contrast-enhanced subiliac, popliteal, and sciatic lymph nodes and cauterize the lymphatic vessels. Next, an approximately 10-mm-wide strip of inguinal region skin was excised circumferentially and the proximal side of that wound cauterized. The distal side was fixed to the myofascia using 6-0 nylon sutures at four different sites. Antibiotics ointment for preventing wound infection was not used in this study. Two mice were bred in a cage after surgery for avoiding fighting. The mice that underwent this procedure were classified as in the new model group.

Surgery for Creating Published Hind Limb Lymphedema Models and a Negative Control Model

As shown in Table 1, some lymphedema animal models are characterized by the combination of the

Table 1. Published Hind Limb Lymphedema Animal Models

Author/Reference	Characteristics of the Procedure		Operation Time	Outcome
Triacca[9]	✓	Lymph node excision (P, IN)	N/A	N/A
	✓	Irradiation		
Nakajima et al[10] (model A)	✓	Lymph node excision (P, IN, IL)	N/A	N/A
Harb et al[11]	✓	Circumferential incision of skin with dressing treatment and fascia fixation	N/A	N/A
	✓	Lymph node excision (IN)		
	✓	Irradiation		
Jorgensen et al[12]	✓	Circumferential incision of skin with dressing treatment and fascia fixation	90 min	Five percent or more increase in volume compared to contralateral hind limb
	✓	Ligation or ablation of lymphatic vessels		
	✓	Lymph node excision (P, IN)		
	✓	Irradiation		
Will et al[1]	✓	Circumferential incision of skin with dressing treatment and fascia fixation	N/A	Ten percent or more increase in volume compared to contralateral hind limb
	✓	Ligation or ablation of lymphatic vessels		
	✓	Lymph node excision (P, IN)		
Iwasaki et al[2]	✓	Circumferential incision of skin with dressing treatment and fascia fixation	N/A	N/A
	✓	Ligation or ablation of lymphatic vessels		
	✓	Lymph node excision (P, IN)		
Roh et al[13] (model B)	✓	Inguinal skin incision without skin excision	N/A	N/A
	✓	Ligation or ablation of lymphatic vessels		
	✓	Lymph node excision (P, IN)		
	✓	Irradiation		
Bramos et al[14]	✓	Circumferential incision of skin with dressing treatment and fascia fixation	N/A	Five percent or more increase in foot pad thickness compared to the contralateral hind limb
	✓	Ligation or ablation of lymphatic vessels		
	✓	Lymph node excision (P)		
Oashi et al[15]	✓	Circumferential incision of skin with fascia fixation	90 min	N/A
	✓	Ligation or ablation of lymphatic vessels		
	✓	Lymph node excision (P, SU)		
	✓	Irradiation		

IL, iliac lymph node; IN, inguinal lymph node; N/A, not available; P, popliteal lymph node; SC, sciatic lymph nodes; SU, subiliac lymph node.

procedures, including lymph node excision, circumferential skin incision, ligation/ablation of lymphatic vessels, or irradiation were previously published. Among them, two control groups of hind limb lymphedema models were prepared from the point of reproducibility. [**See figure, Supplemental Digital Content 2**, which displays the procedure for inducing hind limb lymphedema in positive controls and lymphatic flow. Procedure involving dissection of iliac, popliteal, and inguinal lymph nodes (model A) and procedure involving dissection of inguinal (superficial and deep) and popliteal lymph nodes with cauterization of lymphatic vessels and closure without skin resection (model B), **http://links.lww.com/GOX/A10**.]

One model comprised only excision of popliteal, inguinal, and iliac lymph nodes.[10] The other involved excision of the inguinal (superficial and deep) and popliteal lymph nodes with cauterization of lymphatic vessels and closure without skin excision.[13] They were defined as models A and B, respectively. The mice in the negative control model underwent skin incisions but no lymphedema-inducing procedures.

Measurements of Thigh Circumference and Volume of Hind Limb

Lymphedema was evaluated by measuring volume of the hind limb using a water displacement method,[10,16,17] and circumferences of the hind limb in the femoral region. We defined achievement of lymphedema as any increase in circumference or over 10% increase in the volume of the lower limb compared with before surgery.

Histological Assessment of Hind Limbs

The hind limbs were assessed histologically to determine the number, maximum short-axis diameter, and total area of lymphatic vessels. For comparison between models, samples were excised from four categories of mice (new model, model A, model B, negative control) on postoperative days (PODs) 7, 14, and 28. To determine the effectiveness of MSC transplantation, samples were excised from three categories of mice (new model, MSC transplantation, negative control) on PODs 7, 14, and 28. The samples were fixed in 10% formaldehyde, embedded in paraffin, and cut into 3-µm-thick sections. They were then subjected to heat-induced epitope

retrieval and blocking processes. All slides were incubated with Blocking One Histo (Nacalai Tesque, Kyoto, Japan) at room temperature before incubation with the primary antibody purified hamster anti-podoplanin (1:100; BioLegend, San Diego, Calif.) to detect lymphatic vessels and the secondary antibodies goat anti-hamster IgG (H + L) Alexa Fluor 546 (Invitrogen, Carlsbad, Calif.). Images were acquired using a BZ-X700 fluorescence microscope (Keyence, Itasca, Ill.).

MSC Transplantation

We did not isolate and collect MSCs from the mice. Instead, mouse MSCs were purchased from Cyagen Biosciences [OriCell Strain C57BL/6 mouse mesenchymal cells (Lot # 180078-15); Santa Clara, Calif.]. The MSCs were used after eight passages in this study. These cells were maintained in OriCell mouse mesenchymal growth medium (Cyagen Biosciences).

Before transplantation of MSCs, we assessed the characteristics of the cells as stem cells, which harbor multipotency and enable to produce cytokines/growth factors (ie, paracrine effect). Regarding multipotency, we attempted to induce differentiation into adipocytes and osteoblasts using an adipocyte differentiation kit (Bio Future Technology, Tokyo, Japan) and an osteoblast differentiation kit (Bio Future Technology). Detection of adipocytes and osteoblasts were performed by Oil Red O and Alizarin Red S (Bio Future Technology) staining, respectively. Paracrine effect of the MSCs was assessed by measurement of vascular endothelial growth factor (VEGF) secreted from the cells. In detail, 1.0×10^4 MSCs were cultured for 96 hours. Then, the supernatants of the culture medium were collected and the amount of VEGFA in the supernatants were measured using enzyme-linked immunosorbent assay (ELISA) kit (R&D Systems Quantikine ELISA Kit: Bio-Techne Corp., Minneapolis, Minn.). As a control, the amount of VEGFA in the same culture medium without cells was measured (defined as "no cells").

The MSCs were transplanted on the day of lymphedema induction by injecting them {1×10^6 cells in phosphate-buffered saline [Thermo Fisher Scientific (Gibco), Tokyo, Japan} in a total volume of 100 μL with a 27-gauge needle into three points in the femoral muscle under isoflurane-induced general anesthesia (isoflurane; Fujifilm Wako Pure Chemical Corporation). As a control, the mice, which received induction of lymphedema by the new model method and were injected with the same volume of phosphate-buffered saline without MSCs, were prepared (new model).

Statistical Analysis

All values are presented as mean ± standard error of the mean. Statistical assessments were determined by Student t test for comparing two groups, post-hoc Tukey HSD test for multiple comparisons, and two-way analysis of variance for blood flow assessment. A P value less than 0.05 was considered to denote significant differences. All analyses were performed using SPSS v.24 (IBM, New York, N.Y.).

RESULTS

Hind Limb Lymphedema Induced by the New Procedure Was Longer Lasting

We first studied in detail the anatomy of lymphatic vessels and nodes in mouse hind limbs. Mouse hind limbs have three major lymphatic routes: the subiliac route, which runs through the dermis and flows into the subiliac lymph nodes (Fig. 1A); the popliteal route, which runs posteriorly and flows into the gluteal muscle via the popliteal and sciatic lymph nodes and the inguinal route, which runs through the superficial regions of the hind limb via the inguinal lymph nodes and flows into the abdominal cavity (Fig. 1A).[10] [**See figure, Supplemental Digital Content 3**, which displays the anatomy of lymphatic vessels in the mouse hind limb. Popliteal (yellow arrows) and inguinal (blue arrows) routes, **http://links.lww.com/GOX/A11**] Labeling lymphatic vessels using Evans blue confirmed that subiliac and popliteal routes run through the dermis and the inguinal route flows into fascia between the femoral muscles in the femoral region (Fig. 1A).

The new method entails complete elimination of the three major lymphatic routes in the femoral region with dissection of regional lymph nodes, including subiliac, popliteal, and sciatic lymph nodes. Figure 1B and the bottom of **Supplemental Digital Content 1** (**http://links.lww.com/GOX/A9**) are postoperative photographs. The average surgical time was 14.4 ± 1.3 minutes (n = 20).

We induced lymphedema by three different procedures, including the new one. Lymphedema was achieved without infection within 28 days in all the mice in the new model, model A and model B. (**See figure, Supplemental Digital Content 4**, which displays the changes in the hind limbs of mice in the new model, model A, model B, and the negative control groups. The changes were followed up till POD 28. Dotted circle indicates lymphedema, **http://links.lww.com/GOX/A12**.) In the new model group, lymphedema was detected in the right hind limb on POD 3. The volume of the hind limbs increased gradually over time, reaching a peak on POD 14 and being maintained until POD 28 (Fig. 2A, **Supplemental Digital Content 4**, **http://links.lww.com/GOX/A12**). In contrast, the lymphedema was milder in both models A and B than in the new model, especially regarding model A. The lymphedema reached a peak on POD 7 and had completely resolved by POD 28 in both models A and B (Fig. 2A; **Supplemental Digital Content 4**, **http://links.lww.com/GOX/A12**). The femoral circumference and hind limb volume were consistently highest in the new model group, both in terms of the measured value and ratio to measurements on POD 0. There were some significant differences between the new model and models A and B (Fig. 2B and 2C). In particular, the ratios of both femoral circumference and hind limb volume in the new model group were over 100% during the study period (Fig. 2B and 2C). The ratio of femoral circumference and hind limb volume on POD 28 in the new model group were 115.6 ± 8.1% (versus model A: $P < 0.05$; model B: $P < 0.05$; negative control; $P < 0.05$) and 177.6% (versus model A: $P < 0.01$; model B: $P < 0.05$; negative control; $P < 0.01$), respectively.
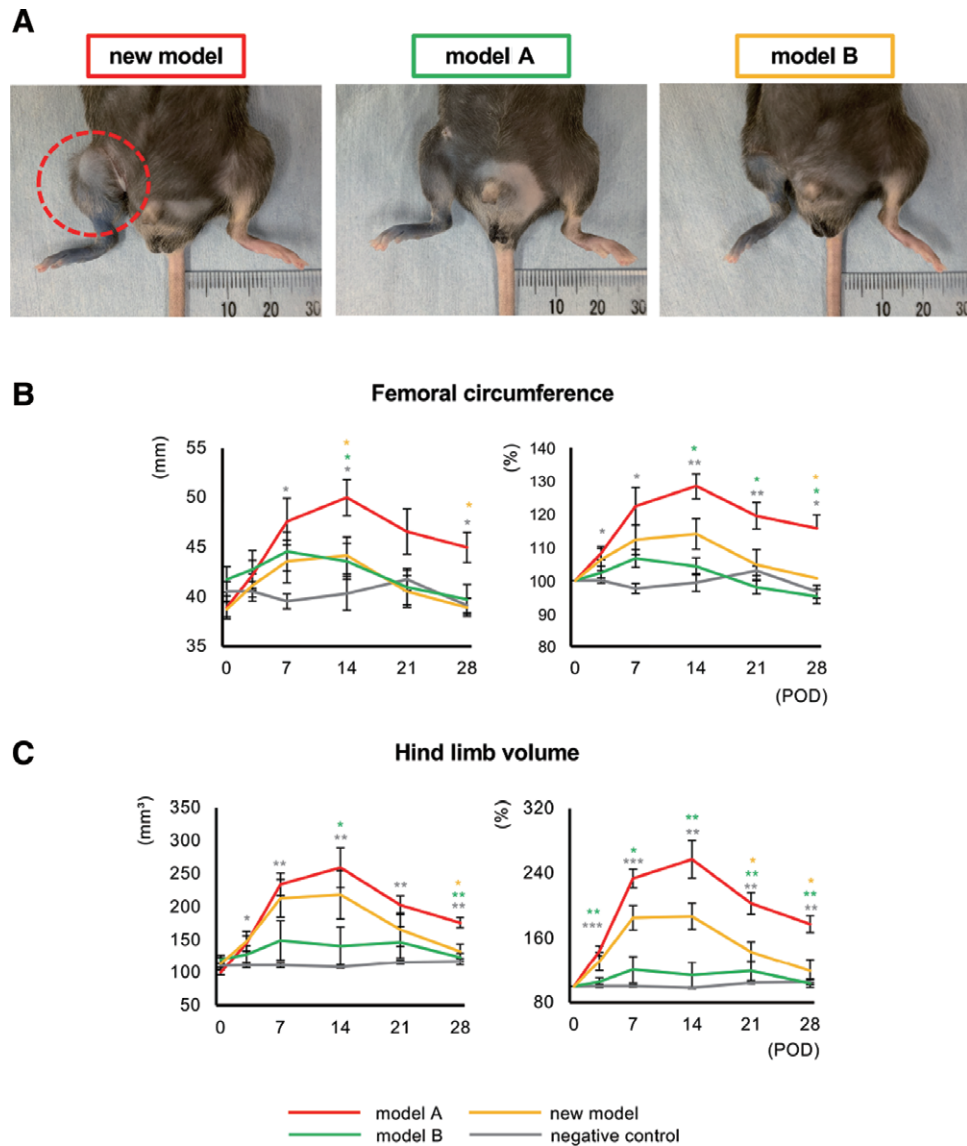
Fig. 2. Assessment of lymphedema after surgery. A. Hind limbs of mice in the new model, model A, model B and the negative control groups on POD 28. Dotted circle indicates lymphedema. B and C, Femoral circumference (B) and hind limb volume (C) in the new model (red), model A (green), model B (yellow), and negative control (gray) groups. Left panel: measured values. Right panel: ratios of data on POD 0. (n = 5 in each group, *$P < 0.05$, **$P < 0.01$, ***$P < 0.001$).

Prominent Dilation of Lymphatic Vessels and Thickening of Subcutaneous Tissue in the New Model

Immunofluorescence staining for podoplanin revealed lymphatic vessels in thigh specimens from all groups. [**See figure, Supplemental Digital Content 5**, which displays the histological images of lymphatic vessels in lymphedema. Immunofluorescence staining for podoplanin (red) in thigh samples obtained from mice in the new model, model A, model B, and the negative control groups on PODs 7, 14, and 28. The yellow arrows indicate podoplanin-positive lymph vessels. Scale bars: 100 μm, **http://links.lww.com/GOX/A13**.] Almost the same number of lymphatic vessels was in each group (data not shown); however, many dilated lymphatic vessels were detected in

the new model. Furthermore, both maximum short-axis diameter and total area of lymphatic vessels (measures for assessing degree of dilation) were higher in the new model group on PODs 7 and 14 than in the other three groups, especially maximum short-axis diameter on POD 14 (versus model A: $P < 0.05$; model B: $P < 0.05$; negative control group: $P < 0.05$; Fig. 3).

We next measured the skin thickness in all groups by examining hematoxylin–eosin-stained thigh specimens and found that the skin was thickest in the new model group, the epidermis being significantly thicker in both the new model and model B groups than in the other two groups (Fig. 4A and 4B). (**See figure, Supplemental Digital Content 6**, which displays the histological
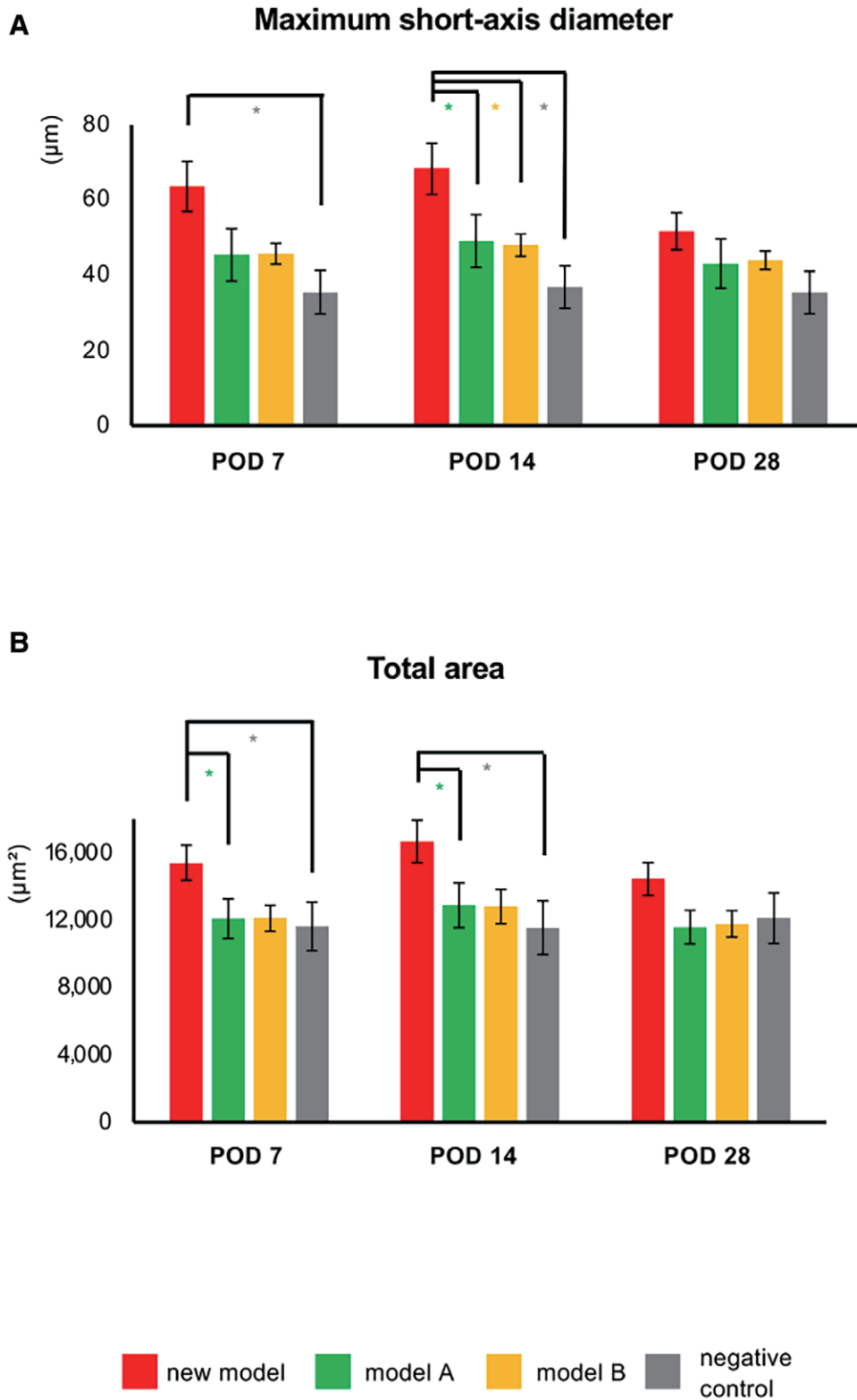
Fig. 3. Assessment of lymphatic vessels in lymphedema. A and B, Maximum short-axis diameter of lymph vessels and total area of lymphatic vessels in the negative control (gray), new model (red), model A (green), and model B (yellow) groups. n = 10, *$P < 0.05$, **$P < 0.01$.

images of skin in the new model. Hematoxylin–eosin-stained thigh specimens in the new model, model A, model B, and negative control groups. The dermis and subcutaneous regions are indicated by magenta and pale blue arrows, respectively. Scale bars: 200 μm, **http://links.lww.com/GOX/A14**.) We found increases in
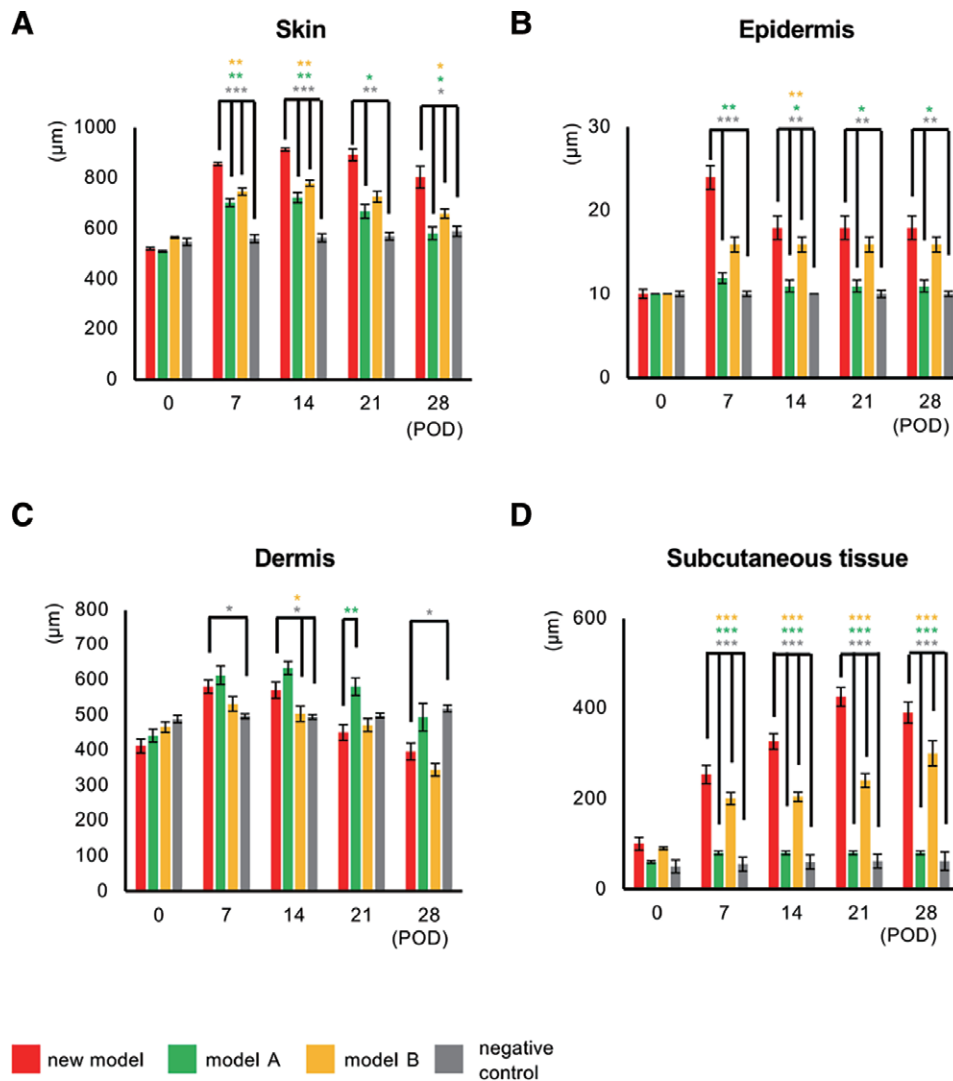
Fig. 4. Assessment of skin thickness in the new model. Thickness of skin (epidermis + dermis + subcutaneous tissue; (A), epidermis (B), dermis (C), and subcutaneous tissue (D) in the new model (red), model A (green), model B (yellow) and negative control (gray). n = 5 in each group, * $P < 0.05$, **$P < 0.01$, ***$P < 0.001$.

dermal thickness in all three lymphedema models (new model, models A and B) on PODs 7 and 14 (Fig. 4C). However, the thickness decreased in the new model group after POD 14 and had returned to basal levels by POD 28 (**Supplemental Digital Content 6, http://links.lww.com/GOX/A14**, Fig. 4C). In contrast, the subcutaneous region became thicker by POD 28 than in the other three groups (versus model A: $P < 0.001$; model B: $P < 0.001$; negative control: $P < 0.001$; Fig. 4D).

New Model Suitable for Assessing the Therapeutic Effects of MSC Transplantation

Finally, we assessed whether our new model is a validated and reliable animal model of lymphedema when it comes to assessing the effects of syngeneic MSC transplantation. The MSCs we used in this study enabled differentiation into both adipocytes and osteoblasts. [**See figure, Supplemental Digital Content 7**, which displays the differentiation and

proliferation potencies of MSCs. Upper and middle panels: Oil Red O and Alizarin Red S stainings. Lower panel: level of cytokines secreted by MSCs. The level of VEGFA in cultured medium with MSCs and no cells. The levels are expressed per 1×10^4 cells. Data are expressed as mean ± SEM (n = 6 in each group, ***$P < 0.001$). **http://links.lww.com/GOX/A15**] Furthermore, these cells secreted VEGF. The level of VEGFA in MSCs was significantly higher than No cells ($P < 0.0001$; **Supplemental Digital Content 7, http://links.lww.com/GOX/A15**).

Supplemental Digital Content 8 shows the changes in hind limb lymphedema in the new model with and without MSC transplantation. (**See figure, Supplemental Digital Content 8**, which displays the changes in the hind limbs of mice in the new model after MSC transplantation. The changes were followed up till POD 28. Dotted circle indicates improved lymphedema, **http://links.lww.com/GOX/A16**).

Although lymphedema was maintained in the new model group, its onset was prevented by MSC transplantation. We did not detect increases in femoral circumference or hind limb volume in the MSC transplantation group, both as measurements and as ratios of these values on POD 0 (**Supplemental Digital Content 8**, http://links.lww.com/GOX/A16, Fig. 5A and 5C). Histological assessment revealed a significantly greater number of lymphatic vessels in the MSC transplantation group than in the new model group after POD 14 (Fig. 6A). [**See figure, Supplemental Digital Content 9**, which displays the histological images of lymphatic vessels in lymphedema after MSC transplantation. Immunofluorescence staining for podoplanin (red) in the thigh samples obtained from mice in the new model and MSC transplantation groups on PODs 7, 14, and 28. The yellow arrows indicate the podoplanin-positive lymph vessels. Scale bars: 100 µm. http://links.lww.com/GOX/A17.) Both maximum short-axis diameter and total area of lymphatic vessels were also greater in the MSC transplantation group (Fig. 6B and 6C).

DISCUSSION

Most published lymphedema animal models have incorporated a combination of circumferential incision of the skin with fascia fixation, ligation or ablation of lymphatic vessels, lymph node dissection, and/or irradiation.[1,2,11–16] Although these measures are potent and critical for induction of lymphedema, few publications reported maintaining lymphedema for over a month without irradiation or dressing. We therefore aimed to develop a simple but reliable and long-lasting hind limb lymphedema model that would reflect the dynamics of foot lymphedema induced by surgery for malignant diseases such as uterine and ovarian cancer[18] and be easy to reproduce and apply widely. We chose not to use irradiation to achieve our goal because it is invasive, induces inflammation and fibrosis, and does not reliably induce persistent lymphedema.[8]

We concluded that complete elimination of lymphatic systems in the femoral region is required for developing a long-lasting lymphedema model. To achieve this, we first studied the anatomy of mouse lymph nodes and lymphatic routes in detail.[19] We clarified the 3D anatomy of lymphatic routes in this study. These findings were critical for developing a procedure for inducing lymphedema that comprised radical elimination of the lymphatic system. We succeeded in eliminating it completely by making a circumferential skin incision with fascia fixation and cauterization of the skin to interrupt the subiliac and popliteal routes, complete dissection of regional lymph nodes, and ablation of the inguinal route. This procedure achieved hind limb lymphedema that persisted for at least a month. In our model, the subcutaneous tissue remained thickened with dilation of lymphatic vessels throughout the observation period. We postulated that elimination of both dermal lymphatic routes (subiliac and popliteal routes) and the inguinal route prevents drainage of interstitial fluid, which then pools, mainly in subcutaneous

tissue. This fluid could not be absorbed into peripheral lymphatic vessels because we succeeded in eliminating the main lymphatic routes. Furthermore, our detailed understanding of the lymphatic anatomy likely contributed to shortening the operation time. The average operation time of this new model is shorter than reported for previous models.[12,15] The shorter operation time may have contributed to minimizing adverse events, including infection, ischemia of the foot, and other life-threatening complications.[20,21]

We also assessed the validity and reliability of this model by determining the therapeutic effect of MSC transplantation. Although the lymphedema induced in the new model lasted a month, there was no evidence of lymphedema in the mice in the new model that underwent syngeneic MSC transplantation. MSCs contribute to lymphangiogenesis via differentiation into lymphatic endothelial cells and production of some growth factors.[13] Our previous studies have revealed that transplanted syngeneic and xenogeneic MSCs promote both angio- and lymphangiogenesis via promoting angio- and lymphangiogeneic factors and contribute to cure of ischemic hind limbs and diabetic ulcers in animal models.[22,23] Promotion of lymphangiogenesis is a promising strategy for resolving lymphedema via drainage of excessive interstitial fluids from subcutaneous tissue. The therapeutic effects, practicality, and safety of MSC transplantation for lymphedema have been assessed in some animal and clinical studies.[3,4] Although the preferable therapeutic effects of MSCs for lymphedema have been elucidated, it is still unclear which cytokines derived from MSCs harbor a specific effect on improvement of this disease. Further detailed studies are needed.

One limitation of this model is the difficulty in creating lymphedema that lasts for over a month. Achievement of a semipermanent lymphedema model would enable evaluation of the long-term effects of therapy for lymphedema. The development of large animal models of lymphedema, such as nonhuman primates, would be challenging but will likely produce more reliable data than a rodent model. The other reason is the difficulty of making lymphedema animal models which reflect on the permanent lymphedema in humans. Chronic inflammation in lymphatic fluid stasis induces fibrosis, decreases lymphatic pumping, and prevents collateral lymphatic formation, which lead to irreversible lymphedema under lymphatic dysfunction. On the other hand, many animal lymphedema models, including ours, are temporary and recover spontaneously due to prevention of chronic inflammation. Additional therapy which induces chronic inflammation and fibrosis after lymphatic elimination might be necessary for establishing a permanent lymphedema model.

Likely to lymphedema, we also consider that a reliable animal model is important to improve technology of plastic and reconstructive surgery, including skin flaps,[24] wound healing,[25] and other plastic technology,[26] These models might contribute to the management of complication correlated with plastic surgery, such as flap congestion.[24]
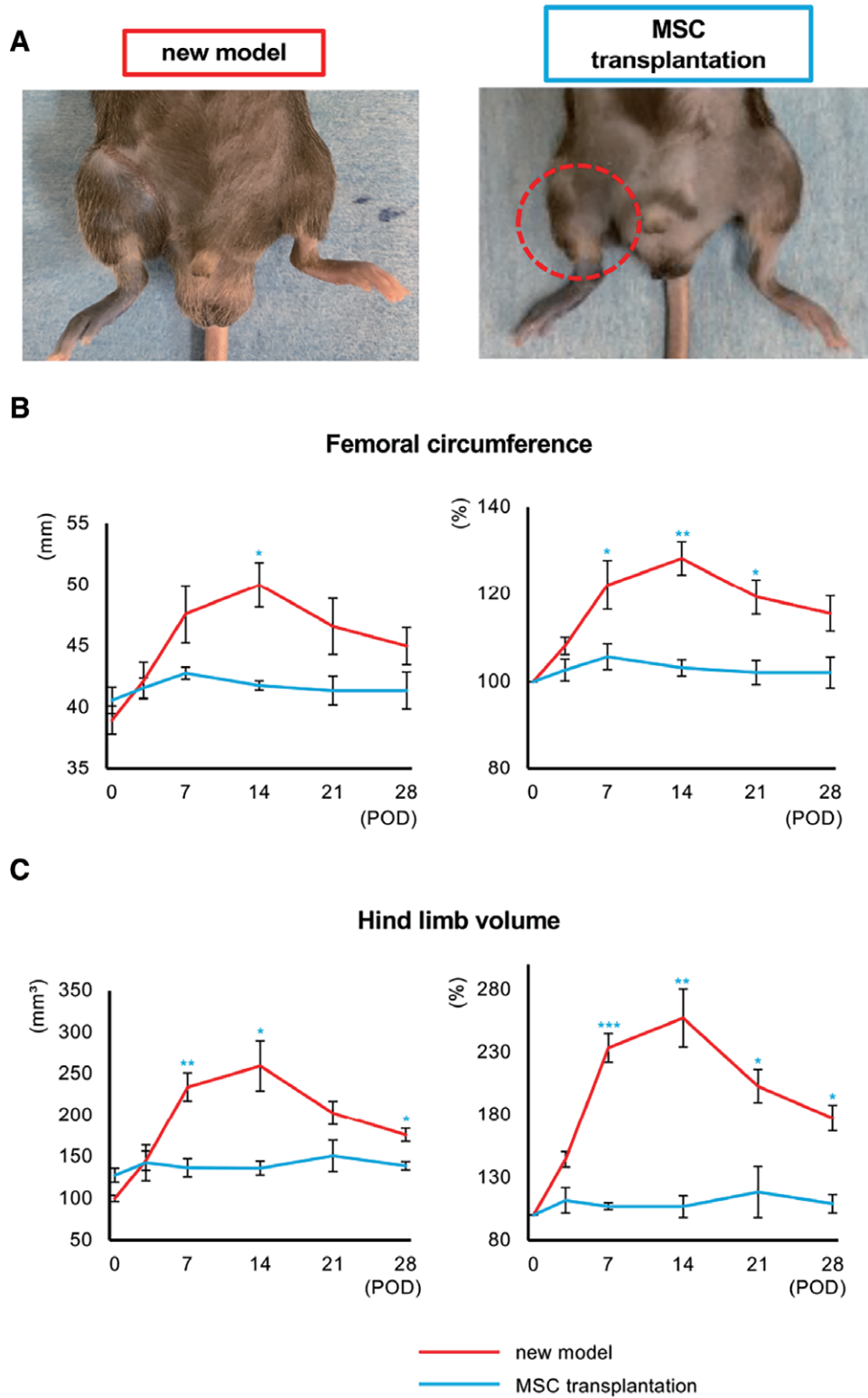
Fig. 5. Assessment of the therapeutic effect of MSC transplantation in the new model. A, Hind limbs of mice in the new model and MSC transplantation groups on POD 28. Dotted circle indicates improved lymphedema. Femoral circumference (B) and hind limb volume (C) in the new model (red) and MSC transplantation (pale blue) groups. Upper panels: measured value. Lower panels: ratios of data on POD 0 (n = 5 in each group, *P < 0.05, **P < 0.01***P < 0.001).

A Number

B Maximum short-axis diameter
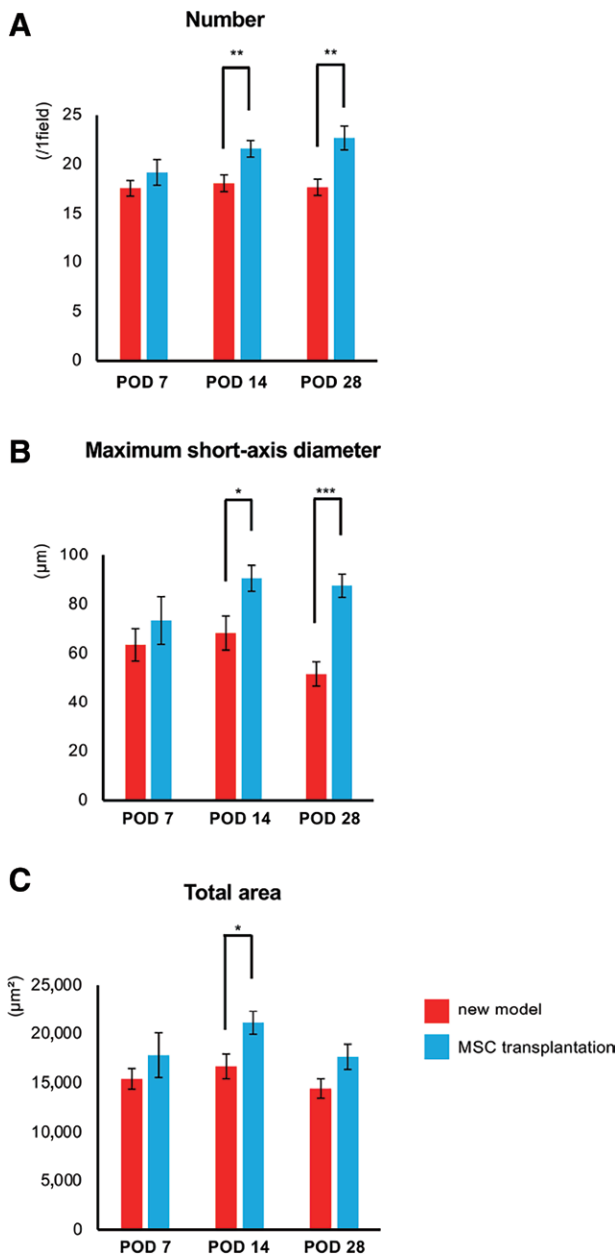
C Total area

Fig. 6. Assessment of lymphangiogenesis following MSC transplantation. The number (A), maximum short-axis diameter (B), and total area of lymphatic vessels (C) in the new model (red) and MSC transplantation (pale blue) groups. n = 10 in each group, *P < 0.05, **P < 0.01***P < 0.001.

In this study, we developed a novel, simple, reproducible, long-lasting mouse lymphedema model. Lymphedema lasting a month was achieved in this model, enabling assessment of the therapeutic effects of MSC transplantation.

Naoaki Sakata, MD and Shohta Kodama, MD
Department of Regenerative Medicine & Transplantation
Faculty of Medicine, Fukuoka University
7-45-1 Nanakuma, Fukuoka 814-0180, Japan
E-mail: naoakisakata@fukuoka-u.ac.jp;
skodama@fukuoka-u.ac.jp

REFERENCES

1. Will PA, Rafiei A, Pretze M, et al. Evidence of stage progression in a novel, validated fluorescence-navigated and microsurgical-assisted secondary lymphedema rodent model. *PLoS One.* 2020;15:e0235965.
2. Iwasaki D, Yamamoto Y, Murao N, et al. Establishment of an acquired lymphedema model in the mouse hindlimb: technical refinement and molecular characteristics. *Plast Reconstr Surg.* 2017;139:67e–78e.
3. Guo Y, Yu Y, Hu S, et al. The therapeutic potential of mesenchymal stem cells for cardiovascular diseases. *Cell Death Dis.* 2020;11:349.
4. Lafuente H, Jaunarena I, Ansuategui E, et al. Cell therapy as a treatment of secondary lymphedema: a systematic review and meta-analysis. *Stem Cell Res Ther.* 2021;12:578.
5. Hsu JF, Yu RP, Stanton EW, et al. Current advancements in animal models of postsurgical lymphedema: a systematic review. *Adv Wound Care (New Rochelle).* 2022;11:399–418.
6. Frueh FS, Gousopoulos E, Rezaeian F, et al. Animal models in surgical lymphedema research—a systematic review. *J Surg Res.* 2016;200:208–220.
7. Kwon S, Janssen CF, Velasquez FC, et al. Radiation dose-dependent changes in lymphatic remodeling. *Int J Radiat Oncol Biol Phys.* 2019;105:852–860.
8. Wang Z, Kim KY, Yoon SH, et al. Radiation inhibits lymph drainage in an acquired lymphedema mouse hindlimb model. *Lymphat Res Biol.* 2020;18:16–21.
9. Triacca V, Pisano M, Lessert C, et al. Experimental drainage device to reduce lymphoedema in a rat model. *Eur J Vasc Endovasc Surg.* 2019;57:859-867.
10. Nakajima Y, Asano K, Mukai K, et al. Near-infrared fluorescence imaging directly visualizes lymphatic drainage pathways and connections between superficial and deep lymphatic systems in the mouse hindlimb. *Sci Rep.* 2018;8:7078.
11. Harb AA, Levi MA, Corvi JJ, et al. Creation of a rat lower limb lymphedema model. *Ann Plast Surg.* 2020;85:S129–S134.
12. Jorgensen MG, Toyserkani NM, Hansen CR, et al. Quantification of chronic lymphedema in a revised mouse model. *Ann Plast Surg.* 2018;81:594–603.
13. Roh K, Cho S, Park JH, et al. Therapeutic effects of hyaluronidase on acquired lymphedema using a newly developed mouse limb model. *Exp Biol Med (Maywood).* 2017;242:584–592.
14. Bramos A, Perrault D, Yang S, et al. Prevention of postsurgical lymphedema by 9-cis retinoic acid. *Ann Surg.* 2016;264:353–361.
15. Oashi K, Furukawa H, Oyama A, et al. A new model of acquired lymphedema in the mouse hind limb: a preliminary report. *Ann Plast Surg.* 2012;69:565–568.
16. Jun H, Lee JY, Kim JH, et al. Modified mouse models of chronic secondary lymphedema: tail and hind limb models. *Ann Vasc Surg.* 2017;43:288–295.
17. Park HS, Jung IM, Choi GH, et al. Modification of a rodent hindlimb model of secondary lymphedema: surgical radicality versus radiotherapeutic ablation. *Biomed Res Int.* 2013;2013:208912.

18. Huang J, Yu N, Wang X, et al. Incidence of lower limb lymphedema after vulvar cancer: a systematic review and meta-analysis. *Medicine (Baltim)*. 2017;96:e8722.

19. Van den Broeck W, Derore A, Simoens P. Anatomy and nomenclature of murine lymph nodes: descriptive study and nomenclature standardization in BALB/cAnNCrl mice. *J Immunol Methods*. 2006;312:12–19.

20. Fogarty BJ, Khan K, Ashall G, et al. Complications of long operations: a prospective study of morbidity associated with prolonged operative time (> 6 h). *Br J Plast Surg*. 1999;52:33–36.

21. Procter LD, Davenport DL, Bernard AC, et al. General surgical operative duration is associated with increased risk-adjusted infectious complication rates and length of hospital stay. *J Am Coll Surg*. 2010;210:60el–65e2.

22. Kuwahara G, Nishinakamura H, Kojima D, et al. Vascular endothelial growth factor-C derived from CD11b+ cells induces therapeutic improvements in a murine model of hind limb ischemia. *J Vasc Surg*. 2013;57:1090–1099.

23. Yamada H, Sakata N, Nishimura M, et al. Xenotransplantation of neonatal porcine bone marrow-derived mesenchymal stem cells improves murine hind limb ischemia through lymphangiogenesis and angiogenesis. *Xenotransplantation*. 2021;28:e12693.

24. Boissiere F, Gandolfi S, Riot S, et al. Flap venous congestion and salvage techniques: a systematic literature review. *Plast Reconstr Surg Glob Open*. 2021;9:e3327.

25. Guarro G, Cozzani F, Rossini M, et al. The modified TIME-H scoring system, a versatile tool in wound management practice: a preliminary report. *Acta Biomed*. 2021;92:e2021226.

26. Winter E, Glauser G, Caplan IF, et al. The LACE+ index as a predictor of 30-day patient outcomes in a plastic surgery population: a coarsened exact match study. *Plast Reconstr Surg*. 2020;146:296e–305e.